

## Comparison of the Structures and Vibrational Modes of Carboxybiotin and *N*-Carboxy-2-imidazolidone

John Clarkson and Paul R. Carey\*

Department of Biochemistry, Case Western Reserve University, 10900 Euclid Avenue, Cleveland, Ohio 44106

Received: October 29, 1998; In Final Form: February 1, 1999

The spontaneous decarboxylation of *N*-carboxy-2-imidazolidone (a model for carboxybiotin) and *N*(1′)-carboxybiotin can be followed at high pH by Raman and FTIR spectroscopies. The major bands associated with vibrations of the carboxylate group have been assigned on the basis of quantum mechanical calculations of *N*-carboxy-2-imidazolidone and *N*(1′)-carboxy-2-methylbiotin. The carboxylate modes are the asymmetric stretch, coupled to the ureido carbonyl stretch, near 1710 cm<sup>-1</sup>, the symmetric stretch near 1340 cm<sup>-1</sup>, and the -CO<sub>2</sub><sup>-</sup> scissoring motion near 830 cm<sup>-1</sup>. In the case of carboxybiotin, the last two modes are strongly coupled with biotin ring modes. All three carboxylate modes disappear as spontaneous decarboxylation occurs, to be replaced by features attributable to the noncarboxylated ring structures. The HF/6-31G\* optimized structure of 2-methylbiotin revealed that the ureido ring portion is essentially planar, in accord with a number of X-ray crystallographic structures of biotin compounds. However, calculations at this level and at the B3LYP/6-31+G(d) level (using density functional theory) predict that the ureido ring in biotin puckers upon carboxylation. Comparison of the structures of carboxybiotin and carboxyimidazolidone, derived at the HF/6-31G\* level, indicates that lengths of the ring-nitrogen-to-carboxylate bonds are equal and that the torsional angles about this linkage are very similar. This strong structural similarity provides a rationale for the observation that, at high pH, the spontaneous rates of decarboxylation of these two molecules are very similar.

### Introduction

Biotin is the critical cofactor for enzymes that transfer units of CO<sub>2</sub> within metabolic pathways.<sup>1</sup> In these enzymes, biotin is covalently attached to the protein at a lysine side chain. Initially, the N1′ position of biotin becomes carboxylated by accepting a CO<sub>2</sub> moiety from a donor molecule at one active site. Carboxybiotin then usually functions as a carrier to deliver CO<sub>2</sub> to an acceptor at a second active site, yielding a carboxylated substrate and regenerating biotin.<sup>1</sup> The detailed mechanism of biotin carboxylation and decarboxylation has engaged the interest of chemists for some time and, although some facets are understood, much remains to be elucidated, particularly at the level of the control of reactivity by protein–biotin interactions. The latter almost certainly has to be invoked to explain, for example, the nucleophilic attack of the N1′ ureido nitrogen on the carboxylate group in some biotin carboxylation steps. Knowles<sup>1</sup> postulated that the reactive N<sup>-</sup> species could be generated by base catalysis at a sufficient rate to account for the observed rate of biotin carboxylation. However, we showed recently that this is not a universal phenomenon. For the biotinylated 1.3S subunit of transcarboxylase, NMR experiments demonstrated that the rate of formation of the N1′<sup>-</sup> species is between 0.14 and 1.4 s<sup>-1</sup> in the physiological pH range 5.5–6.5.<sup>2</sup> These rates are considerably less than the turnover rate of ~66 s<sup>-1</sup> measured for transcarboxylase.<sup>3,4</sup> Other authors have postulated that a transannular interaction involving the biotin ring sulfur atom and the ureido carbonyl could increase the nucleophilicity of the N1′ atom.<sup>5</sup> Although DeTitta and co-workers<sup>6</sup> have summarized the evidence against such an interaction in the relaxed “ground-state” conformation of biotin,

recent calculations by Grant<sup>7</sup> suggest that the sulfur may play a role in activating the N1′ in twisted forms of the biotin molecule that may resemble the transition-state conformation. Again, the twist would result from protein–biotin interactions.

We have instigated a variety of biophysical studies of the enzyme transcarboxylase,<sup>2</sup> which transfers a carboxylate group from methylmalonyl–CoA to pyruvate to form propionyl–CoA and oxalacetate, with the goal of determining the mechanistic chemistry of the carboxylation and decarboxylation reactions. One approach will be to use vibrational spectroscopy to characterize the carboxybiotin species on the enzyme. To support these vibrational analyses, we have undertaken Raman and FTIR studies of the unstable carboxylated intermediates *N*(1′)-carboxy-2-methylbiotin (**2**) and *N*-carboxy-2-imidazolidone (**1**) (shown in Chart 1) in aqueous solutions and in the absence of any protein components. In turn, to understand the vibrational data for the model compounds more fully, we have performed quantum mechanical calculations on the compounds in both their carboxylated and noncarboxylated states (compounds **1–4** in Chart 1).

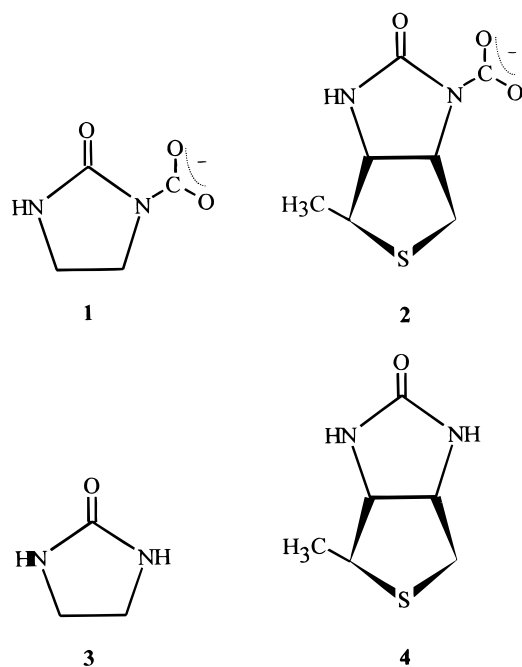
For both model compounds we have been able to identify the major vibrational modes associated with the carboxyl group on the ureido ring and show that these features can be used to follow spontaneous decarboxylation in the Raman or FTIR spectra. In addition to helping establish vibrational assignments, the quantum mechanical calculations provide some insight into the relative stabilities of the high pH forms (where the carboxylate group is ionized) of carboxybiotin and *N*-carboxy-2-imidazolidone.

### Experimental Section

*N*-methoxycarbonyl-2-imidazolidone was synthesized according to Shaeffer’s method<sup>8</sup> as outlined by Caplow.<sup>9</sup> Briefly, 6.88

\* To whom correspondence should be addressed. Phone: 216 368 0031. Fax: 216 368 4544. E-mail: carey@biochemistry.cwru.edu.

CHART 1



g of 2-imidazolidone was heated in 80 mL of chloroform, 12.4 mL of methyl chloroformate were added dropwise, and the mixture refluxed for 40 h. The material was evaporated to dryness under vacuum and recrystallized twice from water.

*N*-carboxy-2-imidazolidone was prepared by adding 0.2 mL of 2 M potassium hydroxide to 1 mL of 0.5 M *N*-methoxycarbonyl-2-imidazolidone. The excess potassium hydroxide ensured rapid production of the carboxylated species and maintained a high pH essential for its stability.

*N*(1')-methoxycarbonylbiotin methyl ester was prepared by refluxing 1 g of biotin methyl ester in 20 mL of chloroform with methyl chloroformate, which had been added dropwise for 24 h.<sup>10</sup> The resulting material was purified by flash chromatography on silica gel eluting with chloroform/methanol 95:5. Carboxybiotin was prepared by adding adding 0.2 mL of 2 M potassium hydroxide to a 1 mL saturated water solution of *N*(1')-methoxycarbonylbiotin methyl ester water solution (approximately 10 mM).

FTIR spectra were obtained using a Bomem MB series FTIR spectrometer, with a CaF<sub>2</sub> cell with a 0.05 mm Teflon spacer, allowing data above 1000 cm<sup>-1</sup> to be obtained. The FTIR samples were dissolved in D<sub>2</sub>O, and potassium deuteroxide was used to prepare the carboxylated species and maintain a high pH.

Raman spectra were obtained using 488 nm excitation from a Coherent Innova 90 argon ion laser and collected on a 0.5 m Spex single monochromator equipped with a Princeton Instruments CCD camera and a Kaiser Optical Systems holographic notch filter, as described in Kim et al.<sup>11</sup>

Ab initio HF/6-31G\* calculations for compounds 1–4 (Chart 1) were carried out with Turbomole (Biosym/MSI, San Diego, CA). Density functional theory (DFT) calculations were carried out with Turbomole for 1 using the adiabatic connection method,<sup>12</sup> ACM functional, and the 6-31G\*\* basis set. DFT calculations for 2 were performed using the B3LYP<sup>13</sup> functional, which is part of the Gaussian 94<sup>14</sup> suite of programs with the 6-31+G(d) basis set, which is recommended for charged molecules.<sup>15</sup> The calculations were performed on a Cray Y-MP8E at the Ohio supercomputer facility.

## Results and Discussion

**Geometries of 2-Imidazolidone and *N*-Carboxy-2-imidazolidone.** Using MP2/6-31G\* ab initio calculations, Musashi and co-workers<sup>16</sup> have recently investigated the utility of *N*-carboxy-2-imidazolidone as a model for carboxybiotin. They predicted that the ring in noncarboxylated 2-imidazolidone (3) is planar, thus resembling the ureido ring in biotin. In contrast, our HF/6-31G\* calculations predict that the structure of the imidazolidone is nonplanar, e.g., the N1–C4–C3–N3 torsional angle is 10° (torsional angles are listed in Table 1, while bond lengths and valence angles are shown in Figure 1). The prediction of nonplanarity is in accord with microwave and theoretical studies on ring puckering and inversion of 2-imidazolidone, which proceeds via a C<sub>2h</sub> conformation.<sup>17</sup> The ring puckering is mainly due to the C3 and C4 methylene groups favoring a staggered conformation. A planar conformation of 3 would maximize the conjugation between the carbonyl and the nitrogen atoms; however, the eclipsing of the methylene C3 and C4 groups is energetically unfavorable. The twist from planarity modeled for 3 resembles that observed in the X-ray crystal structure of dethiobiotin.<sup>18</sup> Our results for the carboxylated form of the ring (1), derived using ACM/6-31G\*\* calculations, are in good accord with the findings of Musashi et al.<sup>16</sup> Both calculations predict that the CO<sub>2</sub> group of 1 is approximately planar with atoms N1–C2–O2, whereas the N3–H bond is markedly displaced from this plane. Moreover, the ring becomes more puckered upon carboxylation. Dihedral angles for selected atoms are given in Table 1. Our calculations demonstrate that the CO<sub>2</sub> group of 1 adopts an unusual geometry with a O–C–O angle of 134° and an extended N–(CO<sub>2</sub>) bond length of 1.523 Å. Musashi et al. observed similar features in their calculation<sup>16</sup> and noted that the CO<sub>2</sub> geometry resembles that of the η<sup>1</sup>-C-coordinated CO<sub>2</sub> ligand in transition metal complexes, such as M[Co<sup>I</sup>(R-slen)(CO<sub>2</sub>)],<sup>19</sup> Rh<sup>I</sup>Cl(diars)<sub>2</sub>–(CO<sub>2</sub>),<sup>20</sup> and Ru(bpy)<sub>2</sub>–(CO)(η<sup>1</sup>-CO<sub>2</sub>).<sup>21</sup>

**Structure and Reactivity: Comparing the Structures of C(2)-Methylbiotin, *N*(1')-Carboxy-2-methylbiotin, and *N*-Carboxy-2-imidazolidone.** The structure of C(2)-methylbiotin (4), computed at the HF/6-31G\* level and summarized in Figure 1, is essentially the same as that predicted by Musashi et al.<sup>16</sup> The ureido ring of 4 is nearly planar with the carbonyl group slightly out of the ureido ring plane. A similar conformation was found in the ureido ring of the 6-31G\* optimized structure and X-ray structure of chainless biotin.<sup>6</sup> Table 1 lists selected dihedral angles of the theoretical structure and compares them to those observed from X-ray structures of dethiobiotin,<sup>18</sup> biotin,<sup>22</sup> and methoxycarbonylbiotin methyl ester.<sup>23</sup> It can be seen that the predicted dihedrals *E* and *F* for 2-methylbiotin are very close to the values for biotin. The addition of the methyl group at C2 introduces a noticeable distortion to the mirror symmetry observed in chainless biotin, with the environments of the ureido, N1', and N3' hydrogen atoms in 4 being distinct. Thus, in Table 1 the dihedral *A* has the opposite sense to *B* (as it does in biotin itself), owing to the C6 methyl group attached to C2. The sulfur ring of 4 constrains the ureido ring to a near-planar conformation, maximizing the conjugation of the ureido carbonyl and nitrogen atoms. This contrasts with the puckered ring predicted for 2-imidazolidone and, in contrast to the conclusion drawn by Musashi et al.,<sup>16</sup> we contend that the latter can only serve as an approximate model for biotin.

The predicted structure of *N*(1')-carboxy-2-methylbiotin (2), summarized in Figure 2 and Table 1, is particularly revealing, both in its comparison to the noncarboxylated form of biotin, to *N*(1')-methoxycarbonylbiotin, and to *N*-carboxy-2-imidazoli-



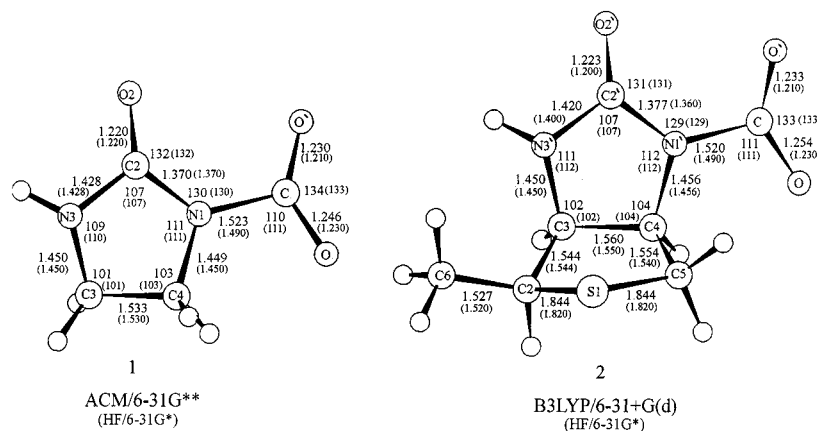


**Figure 2.** Density functional theory optimized structures for *N*-carboxy-2-imidazolidone (**1**) and *N*(1′)-carboxy-2-methylbiotin (**2**).

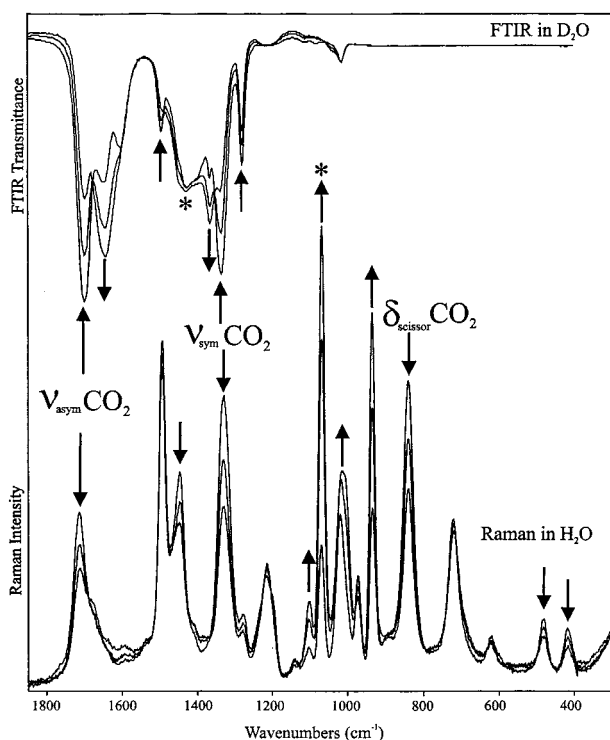


**Figure 3.** Following the spontaneous decarboxylation of *N*-carboxy-imidazolidone by FTIR (top) and Raman (bottom) spectroscopies. In both, experiments data were recorded 10, 40, and 70 min after the addition of KOH (see text).

often be dramatically improved by including solvent molecules in the calculations. It seems likely that a similar improvement could be made here by including solvent effects, especially in light of the fact that the carboxylate group carries a negative charge and solvation will give rise to a redistribution of electron densities in aqueous solution compared to that in vacuo.

**Vibrational Spectra of Carboxybiotin.** Carboxybiotin was prepared at pH 14 in a manner similar to that for *N*-carboxy-2-imidazolidone,<sup>10,24</sup> permitting us to follow the spontaneous decarboxylation by either Raman or FTIR spectroscopy. Figure 5 compares the FTIR spectrum of freshly prepared carboxybiotin with those 0.5 and 1.5 h after preparation; Figure 6 shows the Raman spectra of carboxybiotin freshly prepared and 1 h later.

In Figure 5, the features near 1652 and 1409  $\text{cm}^{-1}$  increase with time and are due to biotin and bicarbonate, respectively. A biotin feature occurs in the first spectrum because by the time these data were recorded, some C–N cleavage had occurred under the conditions used to hydrolyze the ester. The intense

Raman band at 1069  $\text{cm}^{-1}$  in Figure 6 is also due to the production of bicarbonate. The important changes in Figure 5 are the decrease in the peaks near 1701  $\text{cm}^{-1}$  and the doublet near 1320 and 1335  $\text{cm}^{-1}$ . These are mirrored in the Raman spectra by the decrease in the features at 1718 and 1322  $\text{cm}^{-1}$ . The results of the B3LYP/6-31+G(d) calculations, depicted in Figure 7, show that the bands near 1710 and 1320  $\text{cm}^{-1}$  correspond approximately to the carboxylate asymmetric stretch (coupled to the ureido carbonyl) and the symmetric stretch seen for the imidazolidone analogue. One difference, apparent from a comparison of the normal modes depicted in Figures 4 and 7, is that for carboxybiotin the carboxylate symmetric stretch is vibrationally coupled to biotin ring modes, whereas the carboxyimidazolidone mode is more localized.

There are a number of possible explanations as to why the symmetric stretch appears to consist of two features (resolved in the FTIR spectrum and unresolved in the Raman). For example, the mode could be split because of a Fermi doublet-type interaction with a fundamental in the 660  $\text{cm}^{-1}$  region. Another possibility is that significant carboxylation has occurred at the N3′, giving rise to a mixture of N3′ and N1′ carboxylated species. Although both Knappe et al.<sup>10</sup> and Berkessel and Breslow<sup>32</sup> indicated that in their preparations less than 10% of the carboxymethyl groups are at the N3′ position, we plan to explore this issue further by the use of NMR. For carboxybiotin the calculations predict that, as for carboxyimidazolidone, the carboxylate scissoring motion occurs in the 800  $\text{cm}^{-1}$  region and that this motion is significantly coupled to biotin ring modes (Figure 7). The Raman spectra seen in Figure 6 demonstrate that two moderately intense features at 825 and 928  $\text{cm}^{-1}$  decrease as decarboxylation occurs. Again, further work is needed to determine if these bands emanate from a single or from two carboxylated species. Despite this ambiguity, we are able to conclude that the asymmetric, symmetric, and scissoring modes for the carboxylate moiety of carboxybiotin occur in the same regions as for carboxy-imidazolidone. One difference is that, while for carboxybiotin the CO<sub>2</sub> asymmetric stretch, coupled to the ureido carbonyl, is a localized mode, the symmetric and scissoring modes have significant contributions from motions of the biotin ring. The high intensities of the asymmetric stretch in the infrared and of the symmetric stretch in the Raman make these bands leading candidates for probing carboxybiotin sites within proteins. An additional notable feature in the Raman spectra is the intense band near 690  $\text{cm}^{-1}$  (Figure 6). In keeping with the strong Raman scattering properties of C–S linkages, the B3LYP/6-31+G(d) calculations (not shown) assign this band to the S–C(5)–C(4) stretch. This feature may prove useful as a marker for changes in conformation involving

**TABLE 2: Experimental and Calculated Frequencies for the Major Vibrational Modes Associated with the Carboxylate Group<sup>a</sup>**

	experimental (cm <sup>-1</sup> )		calcd	description
	Raman	IR (D <sub>2</sub> O)		
<i>N</i> -carboxy-2-imidazolidone	840		802 (799)	CO <sub>2</sub> scissors, N-C(O <sub>2</sub> ), NH def
	1328	1338	1301 (1301)	CO <sub>2</sub> sym, N-CO <sub>2</sub>
	1712	1701	1893 (1892)	CO <sub>2</sub> asym, C=O
<i>N</i> (1')-carboxy-2-methylbiotin (calcd)	925, 825		765 (763)	CO <sub>2</sub> scissors, ring modes
<i>N</i> (1')-carboxybiotin (exptl)	1322	1334, 1320	1275 (770)	CO <sub>2</sub> sym, ring modes
	1718	1701	1817 (1814)	CO <sub>2</sub> asym, C=O, N-H bend

<sup>a</sup> See Figures 4 and 7 for pictorial representations of the modes. The calculations were undertaken at the ACM/6-31G\* level for *N*-carboxy-2-imidazolidone and at the B3LYP/6-31+G(d) level for *N*(1')-carboxy-2-methylbiotin. Calculated values in parentheses are for the molecules deuterated at N-D, for comparison with experimental IR spectra that are recorded in D<sub>2</sub>O.

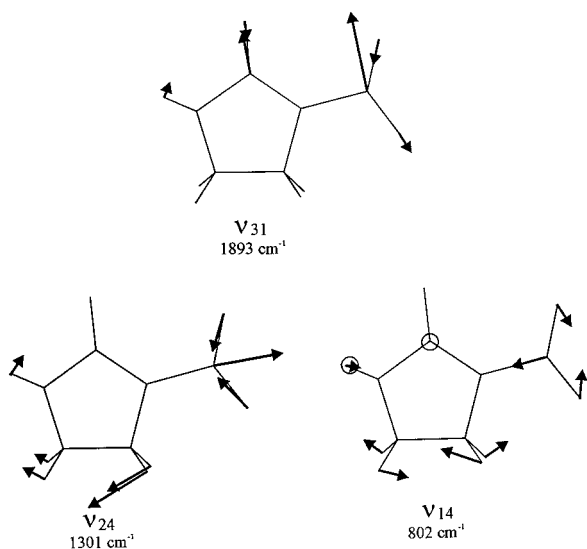


**Figure 4.** Major vibrational modes associated with the carboxylate group in *N*-carboxyimidazolidone. The modes are derived from ACM/6-31G\*\* calculations. Arrows represent atomic displacement vectors during half-phase of vibration, multiplied by approximately 10 times the true value.

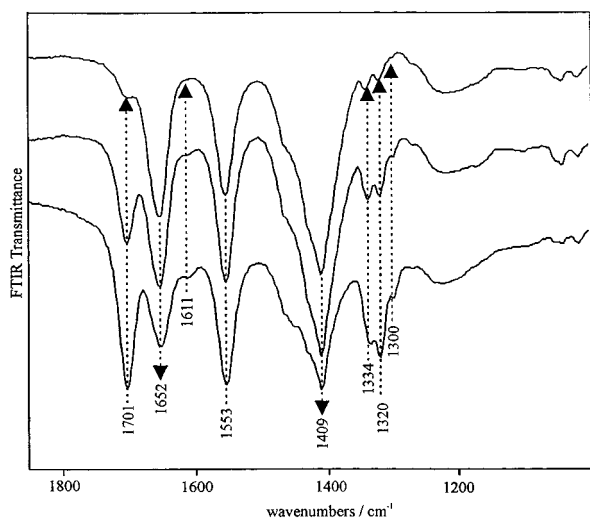


**Figure 5.** FTIR spectra of freshly prepared carboxybiotin (bottom) and after 0.5 h (middle) and 1.5 h (top).

the ring sulfur at protein sites and thus has the potential to provide evidence for the protein-induced distortions proposed by Grant.<sup>7</sup>

## Conclusions

The initial objective of this research was to characterize the FTIR and Raman spectra of the unstable species *N*(1')-

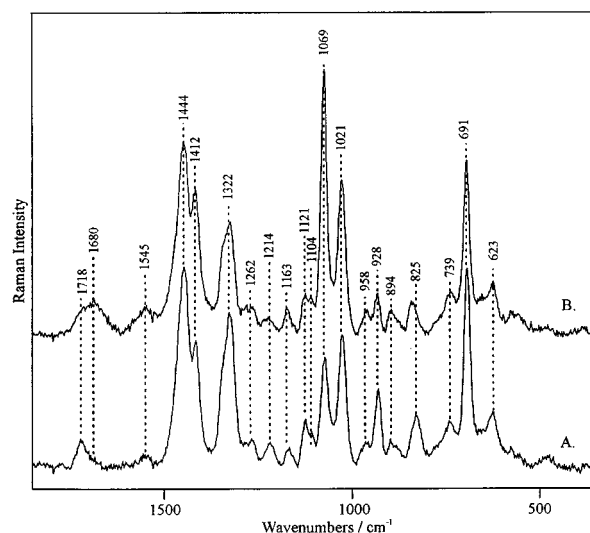


**Figure 6.** Raman spectrum of freshly prepared carboxybiotin (bottom) and after 1 h (top).

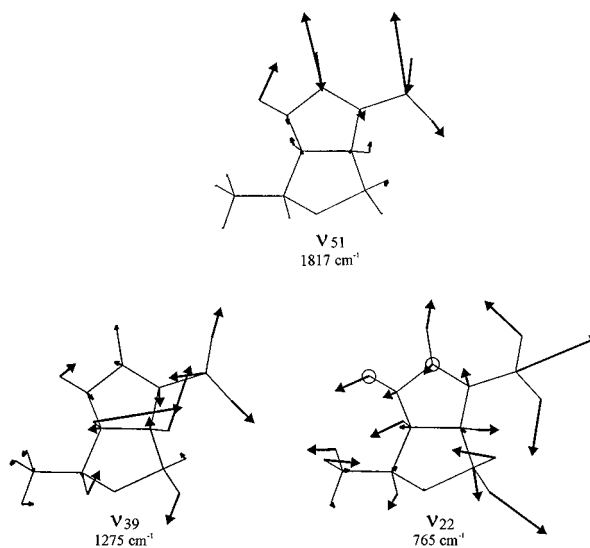


**Figure 7.** Major vibrational modes associated with the carboxylate group in 2-methyl-*N*(1')-carboxybiotin. Arrows represent atomic displacement vectors during half-phase of vibration, multiplied by approximately 10 times the true value. Open circles represent atomic displacement vector out of the plane of the paper toward the reader. Ureido ring is approximately in the plane of the paper.

carboxybiotin and of *N*-carboxy-2-imidazolidone, which serve as simple models for biotin. Good quality vibrational data were obtained for both species. Quantum mechanical calculations were used to define the equilibrium conformations of both carboxylated species and of the parent decarboxylated

compounds. These calculations also allowed us to assign the three major modes associated with the carboxylate groups in the Raman and IR spectra: these are the carboxylate asymmetric stretch, coupled to the ureido carbonyl stretch, near  $1710\text{ cm}^{-1}$ , the symmetric stretch near  $1340\text{ cm}^{-1}$ , and the  $-\text{CO}_2^-$  scissoring mode near  $830\text{ cm}^{-1}$ . The last two are coupled to biotin ring motions in carboxybiotin. All three modes are seen to decrease with time as spontaneous decarboxylation occurs. In future studies this information will serve as a starting point for our interpretation of the vibrational data from carboxybiotin bound to its carrier proteins and involved in carboxylation reactions. Insight has also emerged from the quantum mechanical calculations regarding structure and reactivity. The calculations for the high pH forms of carboxyimidazolidone and carboxybiotin indicate that the structures about the ring-to-carboxylate group are very similar, providing a rationale for the observation that the rates of spontaneous decarboxylation at high pH for the two molecules are very similar.<sup>24</sup>

**Acknowledgment.** The authors are grateful for the support of the NIH (RO1 DK 53053) and the Ohio supercomputer center.

## References and Notes

- Knowles, J. R. *Annu. Rev. Biochem.* **1989**, *58*, 195–221.
- Reddy, D. V.; Shenoy, B. C.; Carey, P. R.; Sonnichsen, F. D. *Biochemistry* **1997**, *36*, 14676–14682.
- Shenoy, B. C.; Xie, Y.; Park, V. L.; Kumar, G. K.; Beegen, H.; Wood, H. G.; Samols, D. *J. Biol. Chem.* **1992**, *267*, 18407–18412.
- Wood, H. G.; Chiao, J.-P.; Poto, E. M. *J. Biol. Chem.* **1977**, *252*, 1490–1499.
- Mildvan, A. S.; Scrutton, M. C.; Utter, M. F. *J. Biol. Chem.* **1966**, *241*, 3488–3498.
- DeTitta, G. T.; Blessing, R. H.; Moss, G. R.; King, H. F.; Sukumaran, D. K.; Roskwitalski, R. L. *J. Am. Chem. Soc.* **1994**, *116*, 6485–6493.
- Grant, A. S. *J. Mol. Struct.: THEOCHEM* **1998**, *422*, 79–87.
- Schaeffer, H. J.; Bhargava, P. S. *J. Pharm. Sci.* **1964**, *53*, 137–143.
- Caplow, M. *J. Am. Chem. Soc.* **1965**, *87*, 5774–5785.
- Knappe, J.; Ringelmann, E.; Lynen, F. *Biochem. Z.* **1961**, *335*, 168–176.
- Kim, M.; Owen, H.; Carey, P. R. *Appl. Spectrosc.* **1993**, *47*, 1780–1783.
- Becke, A. D. *J. Chem. Phys.* **1993**, *98*, 5648–5652.
- Lee, C.; Yang, W.; Parr, R. G. *Phys. Rev. B* **1988**, *37*, 785–789.
- Frisch, M. J.; Trucks, G. W.; Schlegel, H. B.; Gill, P. M.; Johnson, B. G.; Robb, M. A.; Chesseman, J. R.; Keith, T. A.; Montgomery, J. A.; Raghavachari, K.; Al-Laham, M. A.; Zakrzewski, V. G.; Ortiz, T. V.; Foresman, J. B.; Cioslowski, J.; Stefanov, B. B.; Nanayakkara, A.; Challacombe, M.; Cheng, C. Y.; Anala, P. Y.; Chen, W.; Wong, W.; Andres, J. C.; Peplogle, E. S.; Comperts, R.; Martin, R. L.; Fox, D. L.; Binkley, J. S.; DeFrees, D. J.; Baker, J.; Stewart, J. P.; Head-Gordon, M.; Gonzales, C.; Pople, J. A. *Gaussian 94*; Gaussian Inc.: Pittsburgh, PA, 1995.
- Foresman, J. B.; Frich, A. *Exploring Chemistry with Electronic Structure Methods*, 2nd ed.; Gaussian Inc.: 1996.
- Musashi, Y.; Hamada, T.; Sakaki, S. *J. Am. Chem. Soc.* **1995**, *117*, 11320–11326.
- Otero, J. C.; Marcos, J. I.; Lopez-Cantarero, E.; Chacon, A. *Chem. Phys.* **1991**, *157*, 201–207.
- Chen, C.; Parthasarathy, R.; DeTitta, G. T. *J. Am. Chem. Soc.* **1976**, *98*, 4983–4990.
- Fachinetti, G.; Floriani, C.; Zanazzi, P. F. *J. Am. Chem. Soc.* **1978**, *100*, 7405–7407.
- Calabrese, J. C.; Herskovitz, T.; Kinney, J. B. *J. Am. Chem. Soc.* **1983**, *105*, 5914–5915.
- Tanaka, H.; Nagao, H.; Peng, S. M.; Tanaka, K. *Organometallics* **1992**, *11*, 14500–14510.
- DeTitta, G. T.; Edmonds, J.; Stallings, W.; Donohue, J. *J. Am. Chem. Soc.* **1976**, *98*, 1920–1926.
- Stallings, W.; Monti, C. T.; Lane, M. D.; DeTitta, G. T. *Proc. Natl. Acad. Sci. U.S.A.* **1980**, *77*, 1260–1264.
- Tipton, P. A.; Cleland, W. W. *J. Am. Chem. Soc.* **1988**, *110*, 5866–5869.
- Rahil, J.; You, S.; Kluger, R. *J. Am. Chem. Soc.* **1996**, *118*, 12495–12498.
- Saito, Y.; Machida, K. *Bull. Chem. Soc. Jpn.* **1972**, *50*, 359–364.
- Davis, A. R.; Oliver, B. G. *J. Solution Chem.* **1972**, *1*, 329–339.
- Pulay, P.; Forgarasi, G.; Ponger, G.; Boggs, G. E.; Vargha, A. *J. Am. Chem. Soc.* **1983**, *105*, 7037–7047.
- Wong, M. W.; Frisch, M. J.; Wiberg, K. B. *J. Am. Chem. Soc.* **1991**, *113*, 4776–4782.
- Wong, M. W.; Wiberg, K. B.; Frisch, M. J. *J. Am. Chem. Soc.* **1992**, *114*, 523–529.
- Wong, M. W.; Wiberg, K. B.; Frisch, M. J. *J. Am. Chem. Soc.* **1992**, *114*, 1645–1652.
- Berkessel, A.; Breslow, R. *Bioorg. Chem.* **1986**, *14*, 249–261.
- Kapon, M.; Reiser, G. M. *Acta Crystallogr.* **1989**, *C45*, 780–782.